

Microstructure and mechanical properties of Mg–Gd–Y–Zr alloy processed by equal channel angular pressing

ZHANG Fan¹, ZHANG Ke-xiang¹, TAN Cheng-wen^{1,2},
YU Xiao-dong¹, MA Hong-lei², WANG Fu-chi¹, CAI Hong-nian¹

1. School of Material Science and Engineering, Beijing Institute of Technology, Beijing 100081, China;

2. Laboratory of Advanced Materials Behavior Characteristics,
Beijing Institute of Technology and Institute of Space Medico-Engineering, Beijing 100081, China

Received 25 October 2010; accepted 11 January 2011

Abstract: Microstructure evolution and texture development and their effects on mechanical properties of a Mg–Gd–Y–Zr alloy during equal channel angular pressing (ECAP) were investigated. It is found that the microstructure is still inhomogeneous after four passes, and two zones, namely the fine grain zone (FGZ) and the coarse grain zone (CGZ) are formed. The grain refinement occurs mainly by particle-stimulated nucleation (PSN) mechanism, which led to a more random texture after four passes of ECAP. In the ECAP-processed alloy, the strength did not increase while the ductility was enhanced dramatically compared with the as-received condition. The change of ductility of this alloy was discussed in terms of texture and second phase particles.

Key words: Mg–Gd–Y–Zr magnesium alloy; equal channel angular pressing (ECAP); grain size; texture; second phase particles; mechanical properties

1 Introduction

The application of magnesium alloy was greatly limited for its relatively low strength and plasticity. An effective way that can improve the mechanical properties of magnesium alloy is to refine the grains [1–2], which is one of the active research trends. Equal channel angular pressing (ECAP) is a promising and effective severe plastic deformation technique for refining various bulk materials including Mg alloys [3–5]. The method of ECAP has been examined in numerous studies to explore the possibility of inducing previously unobserved structures and properties in a wide variety of metals and alloys [6], and proven to be very effective.

Recently, the ECAP processing to improve the mechanical properties of magnesium alloys through grain refinement and texture changes has been investigated, in which grain refinement and texture modification are both considered to contribute to the great improvement of these properties [7–10]. Rare-earth (RE) containing magnesium alloys exhibit a higher strength compared with the conventional magnesium

alloys due to the solution strengthening. The solution strengthening combined with the grain refinement and texture modification through ECAP offers a potential approach to improve the mechanical properties of magnesium alloys. However, ECAP has been less applied to Mg–RE systems [11–12].

Therefore, in this work, the ECAP was used to modify the microstructure and texture in order to optimize the mechanical properties of a Mg–Gd–Y–Zr alloy. The microstructure evolution and texture modification will be correlated with the mechanical properties.

2 Experimental

The as-received material used in this study was a hot-extruded Mg–Gd–Y alloy having a composition of Mg–11.90Gd–0.81Y–0.44Zr (mass fraction, %). This alloy sheet was machined into rods for ECAP experiment with a diameter of 29 mm and a length of 105 mm. The die was composed of two channels with circular cross-sections, intersecting at an angle of 90° between the entrance and exit channels. ECAP experiments were

conducted on the as-extruded material at 390 °C for one pass, three passes and four passes. The rods were inserted into the die, and held until they reached the pressing temperature, and then they were pressed with a speed of 1 mm/s.

Specimens were cut from the longitude of the as-extruded and ECAP processed materials to examine the microstructure (*Y* plane in Fig. 1). Microstructural analyses were conducted using optical microscope, field emission scanning electron microscope (S-4800 SEM) and transmission electron microscopy (JEOL200CX TEM) operated at 200 kV. Texture evolution during ECAP processes was observed on the *Y* plane. Pole figures were measured using D5000X diffraction instrument. Cylindrical specimens with diameter of 5.0 mm and length of 10.0 mm were machined from both the as-extruded and the ECAP processed rods for compression test, with the compressive axis parallel to the extrusion direction (ED), as shown in Fig. 1. Compressive tests were carried out under a strain rate of $1.0 \times 10^{-3} \text{ s}^{-1}$ at room temperature.

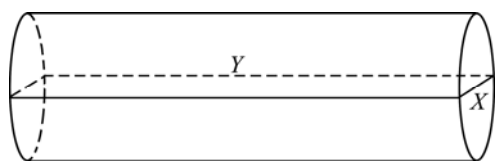


Fig. 1 Schematic illustration of ECAP-processing material

3 Results

3.1 Microstructural characterization

Three-dimensional microstructure of the as-extruded material prior to ECAP is shown in Fig. 2.

The grains in the as-extruded Mg–Gd–Y–Zr alloy are mainly equiaxed, with a linear intercept mean grain size of 18.4 μm , discounting some irregular grains with estimated sizes below 5 μm or strip shape grains larger than 60 μm . Two kinds of residual second phase particles are formed after solution treatment and further hot-extrusion of the as-received material, as shown in

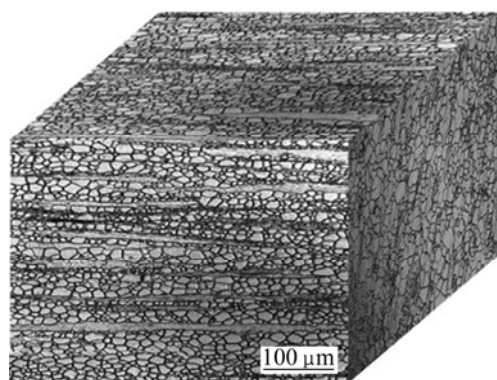


Fig. 2 Initial microstructure of as-extruded Mg–Gd–Y–Zr alloy

Fig. 3(a). The EDS analysis shows that the cubic shaped second phase is rich in Gd and Y while the nearly spherical shaped phase is rich in Zr. The cubic shaped second precipitate phase has been identified as FCC structure with $a=0.56 \text{ nm}$ reported by HE et al [13] and formed in the process of solution treatment, then the distribution of these second phase particles is generally along the extrusion direction during the subsequent hot extrusion, as indicated in Fig. 3(b).

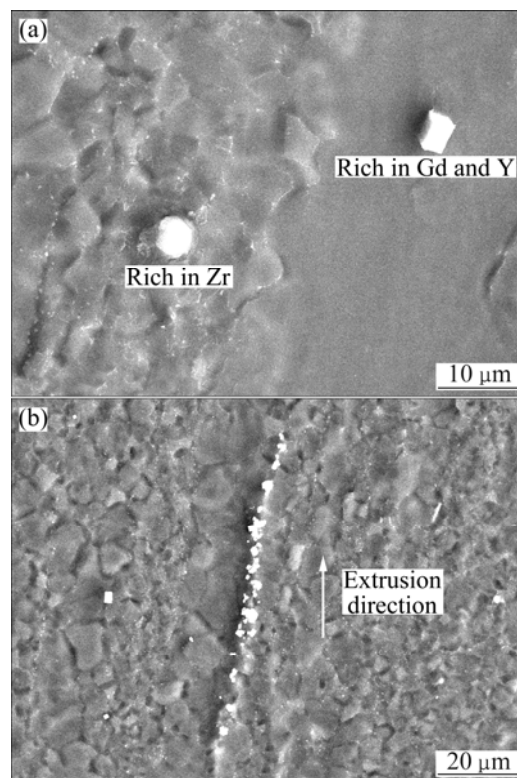


Fig. 3 Two kinds of residual second phase particles (a) and distribution of second phases along extrusion direction (b)

When the material is subjected to ECAP, the alloy would be sheared at the intersection angle of the channel. The result is that the flow line direction and the distribution of second phases changed after ECAP, as shown in Fig. 4, and the inclination angle is approximately 45° compared with the extrusion direction after four passes pressing. The typical metallographs of materials after ECAP one pass, three passes and four passes are shown in Fig. 5. The microstructure is inhomogeneous and large grains are still present up to four passes. It is obvious that the initial homogeneous material is split into a bimodal distribution of two zones: the fine grain zone (FGZ) with grain size of 4–6 μm and the coarse grain zone (CGZ) with grain size of 12–18 μm .

The area fraction of FGZ increases with increasing the number of pass, and its value reaches approximately 45% after four passes of ECAP, as shown in Fig. 6. The average grain size in FGZ is about 5 μm , and the

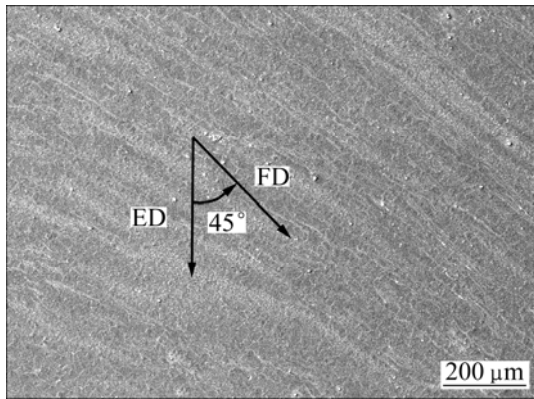


Fig. 4 Direction of both flow line and distribution of second phases varied together by inclination angle of about 45° compared with initial extrusion direction after four passes of ECAP (ED: extrusion direction; FD: flow line direction)

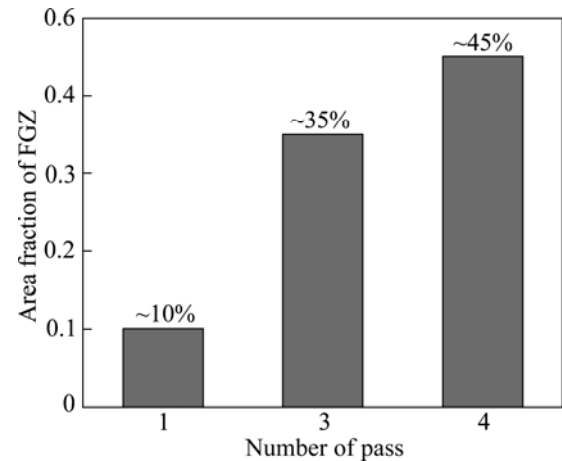


Fig. 6 Area fraction of FGZ vs number of pass

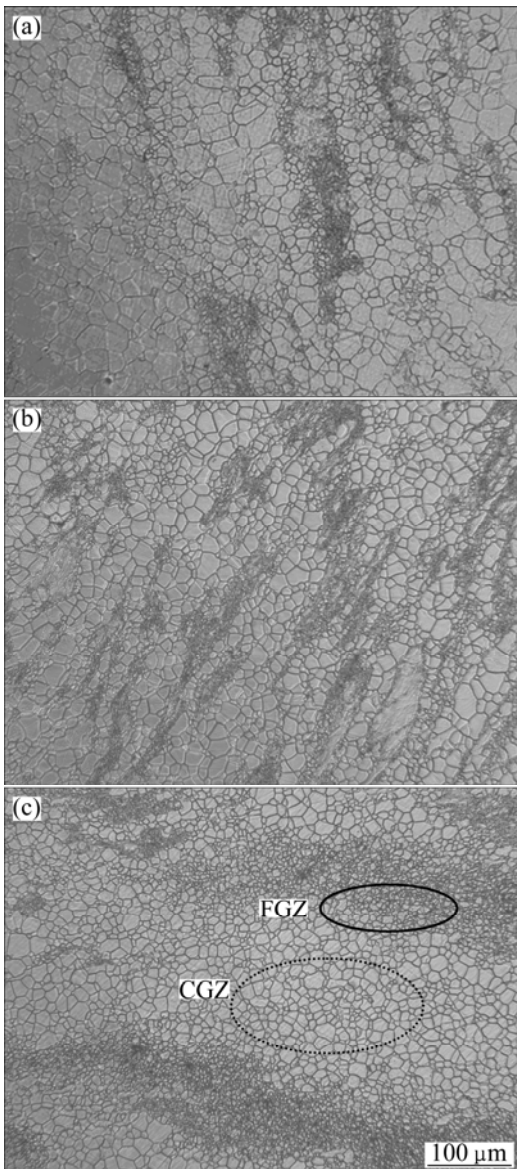


Fig. 5 Typical metallographs of materials after different ECAP passes: (a) 1 pass; (b) 3 passes; (c) 4 passes

variation of the average grain size in CGZ is also limited. Typical microstructures of samples subjected to 1 and 4 ECAP passes are provided in Fig. 7. Two important features can be obtained from this figure. Firstly, the fine grain zones are associated with the distribution of second phase particles for samples after 1 pass and 4 passes. Meanwhile, the area fraction of the fine grain zones increased with increasing the number of pass. Therefore, it is reasonable to speculate that the number of the second phase particles increased with increasing the number of pass. Secondly, the fine grain zones are formed generally around the fine second phase particles. This phenomenon is more obvious for the second phase rich in Gd and Y. In fact, the fine grain zones formed mainly around the fine particles rich in Gd and Y. TEM was used to examine the generality of this observation. Figure 8 shows the fine grain with the size of approximately $5 \mu\text{m}$, forming adjacent to the second phase particle. Those observations suggest that the formation of fine grain zones is directly correlated to the second phase particle.

The pole figures in Fig. 9 (oriented to coincide with the Y plane) present the bulk texture evolution that the Mg–Gd–Y–Zr alloy underwent during ECAP. It is found that the orientation spread of basal planes is broader towards the sheet transverse direction rather than towards the extrusion direction for the as-received hot-extruded material (Fig. 9(a)). In addition, the basal planes in some grains are even parallel to the ED of the sheet. After one pass, the initial texture has developed to a weak $\langle 0001 \rangle$ fiber texture with the c -axis fiber oriented approximately 30° or 45° aft of the vertical axis, as indicated in Fig. 9(b). With the increase of pass number, the $\langle 0001 \rangle$ fiber texture became significantly weaker and a more random texture is formed for the materials processed by three passes and four passes.

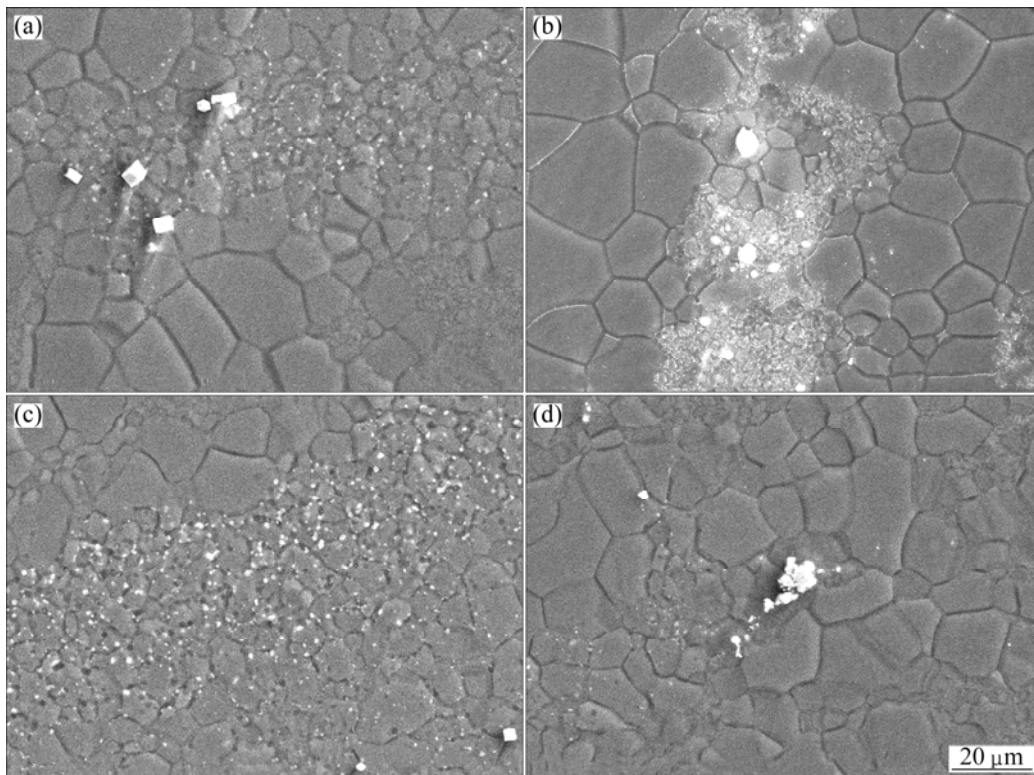


Fig. 7 Typical microstructures of samples subjected to 1 ECAP pass (a, b) and 4 ECAP passes (c, d) (Zones formed around second phase particles rich in Gd and Y (a, c) and rich in Zr (b, d))

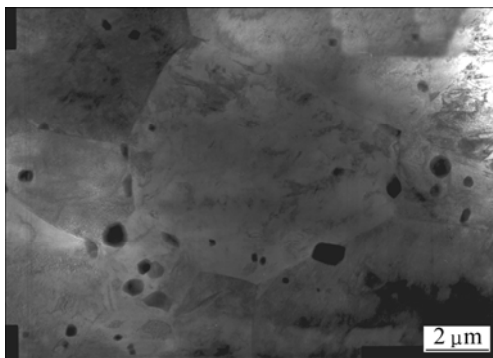


Fig. 8 Fine grain formed adjacent to second phase particles

3.3 Mechanical properties

The true stress—strain curves of the compressive specimens subjected to different passes of ECAP is shown in Fig. 10. It can be observed that the strength decreases while the ductility is enhanced after ECAP compared with the as-received material. The strength decreases dramatically after the first ECAP pass, but is improved pass by pass during the subsequent procedure, while the fracture strain is improved. The yield strength, ultimate compressive strength and fracture strain of different conditions are listed in Table 1. It can be concluded that both the yield strength (YS) and ultimate compression strength (UCS) decrease dramatically after one pass but could be improved pass by pass. In contrast,

the fracture strain is improved by approximately 60% after 1 pass, but decreases slightly during the subsequent ECAP.

Table 1 Yield strength, ultimate compressive strength (UCS) and fracture strain of materials after different passes

Number of pass	$\sigma_{0.2}$ /MPa	UCS/MPa	Fracture strain/%
0	230	412	21.2
1	184	378	34.5
3	207	408	31.2
4	217	420	28.6

4 Discussion

4.1 Mechanism of grain refinement

The grain refinement occurs in the ECAP-processed material by dynamic recrystallization (DRX). The crystallization induced by the effect of the second phase particles is well known and widely observed [14]. The second phase particles have a large effect on the microstructure evolution during plastic deformation, affecting the recrystallisation behavior [14]. If the particles do not plastically deform during deformation, plastic relaxation occurs around the particles to relieve the build-up stress due to the incompatibility in shape between the ‘hard’ particle and

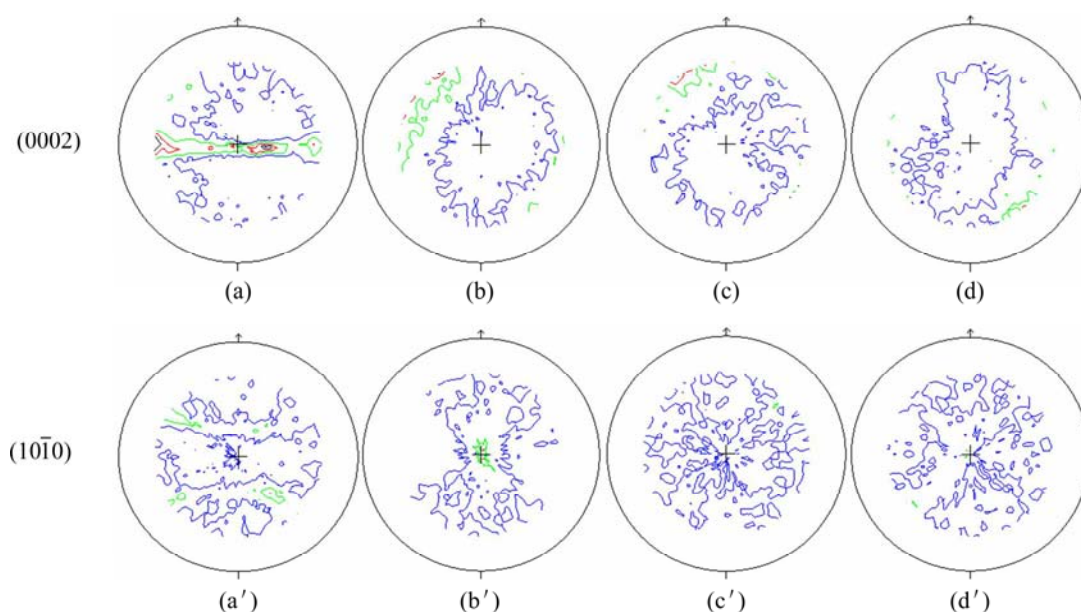


Fig. 9 (0002) and $(10\bar{1}0)$ pole figures of as-extruded (a, a') and ECAP processed alloys after 1 pass (b, b'), 3 passes (c, c') and 4 passes (d, d')

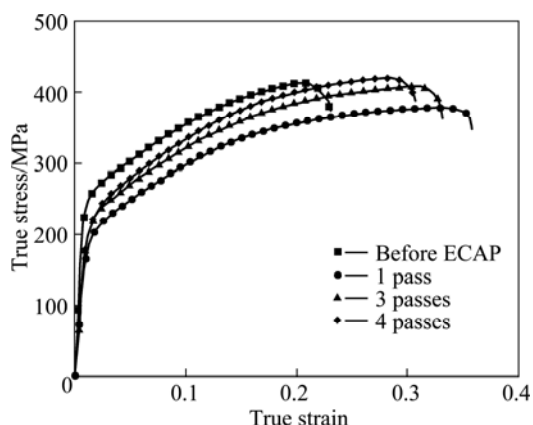


Fig. 10 Compressive true stress—strain curves under different conditions

the plastically deforming matrix [14]. For particles with diameter larger than $0.1 \mu\text{m}$ and high strains, the secondary dislocations caused by stress relaxation will be trapped at the particles, resulting in local lattice rotations in regions adjacent to the particles [15]. These regions are so called deformation zones, and the nucleation of recrystallization may occur within these zones if the strain, strain rate, temperature, particle size and distribution conditions are such that rotated deformation zones are deformed around the particles during plastic deformation [16–17].

This grain refinement mechanism is termed as particle-stimulated nucleation (PSN) and at least one nucleus is formed at each particle, so it is not difficult to understand the fine grain distribution related to the particle distribution. However, as mentioned above, the role of Zr-rich particles is not so obvious compared with

Gd- or Y-rich particles, so it is reasonable to assume that not all of the second phase particles in certain matrix may result in grain refinement or PSN. Investigations by BALL and PRANGNELL [18] showed that when extruded under similar conditions, the distribution of the particles in the ZC71 (Mg–7.2Zn–1.42Cu–0.81Mn, mass fraction, %) alloy does not obviously correlate to grain size distribution as the particles do not act as nucleation sites, while they do in the WE54 (Mg–5.2Y–1.74Nd–0.95RE–0.59Zr) alloy. However, how this difference acts is not well understood.

It is obvious that, in this study, DRX occurred mainly by PSN mechanism due to the widely spread second phase particles especially for particles rich in Gd and Y, leading to the grain refinement.

4.2 Evolution of texture

The textures of the ECAP-processed magnesium alloys have been studied previously [11–12]. The basal plane in the majority of grains will be rearranged to the shearing direction, attributing to the simple shear applied to the material at the intersection of the channels during ECAP. In this study, alloying through additions of Gd and Y may weaken the texture, leading to a weaker texture compared with other magnesium alloys such as AZ31 with a strong $\langle 0001 \rangle$ fiber texture.

With the increase of pass number, the fiber texture became significantly weaker and a more random texture developed compared with the sample after 1 pass. This phenomenon results from the fact that PSN of recrystallization is the main mechanism that may weaken the texture. BALL and PRANGNELL [18] and MACKENZIE et al [19] also proposed that PSN is an

active mechanism contributing to the development of a weaker texture during extrusion of WE54 and WE43 alloy, respectively.

4.3 Effect of microstructure on mechanical properties

The ductility of sample after 1 pass is significantly improved while the strength decreases compared with the as-received material. This fact may be attributed to the unique microstructure of sample after 1 pass. Experimental results show that the variance of average grain size after one pass ECAP is limited (~10% FGZ), and the second phase particle seldom cracks. Therefore, the grain size and second phase particles do not change the mechanical property markedly. Consequently, the texture differences between the 1 pass and the as-received alloys may result in the significantly enhanced ductility, as shown in Fig. 9. The grains in the 1 pass-sample are in a more favorable orientation to accommodate the imposed strain, and the corresponding results are higher ductility and lower strength.

With the increase of pass number, the flow stress markedly increased, whereas the ductility slightly decreased. The improved strength with pass number is associated with the reduction of the grain size, but can not explain the fact that the decrease of fracture strain from 34.5% (1 pass) to 28.6% (4 passes). This is partially attributed to the fact that 1 pass-sample is softer than the 3 or 4 passes-sample, because the former has a preferred orientation for compression strain accommodating along the extrusion axis by the soft deformation mechanisms, namely basal slip of dislocations with $\langle a \rangle$ Burgers vectors. It also seems to be related to changes in the distribution of the second phase particles during ECAP.

A typical SEM image of materials subjected to four passes of ECAP is indicated in Fig. 11. The second phase particles get finer and more widely spread in the matrix with the increase of pass number. This phenomenon may correlate to the fracture behavior, and in turn affects the ductility.

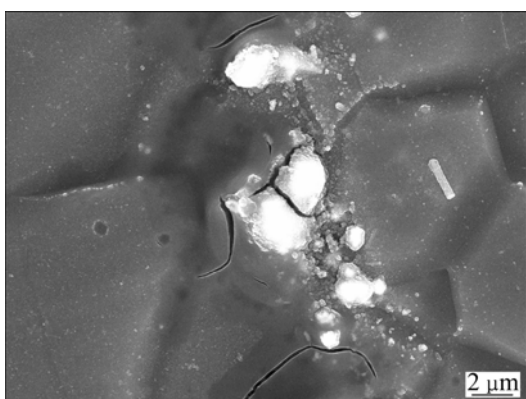


Fig. 11 Micro-cracks formed in four 4 passes-sample

During the ECAP deformation, micro-cracks nucleated at the interface between the second phase particles and the matrix, and cracks are also formed within the second phase particles themselves. These micro-cracks could be macro-crack source during the compressive deformation, which may lead to macroscopic failure. On the other hand, micro-cracks would also nucleate at the interface between the second phases and the matrix during the compression due to the different structure of the second phases (FCC), which is incompatible with the hexagonal structure of the magnesium matrix. Therefore, these micro-cracks formed in the ECAP deformation could be responsible for the slightly decrease in fracture strain after one pass, despite of the grain size getting more and more fine during the subsequent ECAP procedure, which may enhance the ductility.

5 Conclusions

1) The grain size of the Mg–Gd–Y–Zr alloy is inhomogeneous after four passes of ECAP, and two zones, i.e. the fine grain zone (FGZ) and the coarse grain zone (CGZ) are formed during ECAP. The area fraction of FGZ is increased pass by pass, and the value is approximately 45% after four passes of ECAP.

2) The FGZ is greatly related to the distribution of the fragmented fine second phase particles. Inspection shows that the grain refinement occurs mainly by PSN mechanism. PSN of recrystallization resulted in a reduction in texture and a more random texture is developed in the 4 passes-sample.

3) The grain size reduction resulted in the increase of strength with increasing pass number. The enhancement of ductility and decrease in strength were mainly attributed to the texture development, namely the initial texture was decomposed and a more random texture was developed after four passes of ECAP.

4) The decrease of fracture strain from 34.5% (1 pass) to 28.6% (4 passes) was partially attributed to the texture development, and also partially to the wide distribution of second phase particles that are the potential nucleation sites of micro-cracks.

References

- [1] MIYAHARA Y, MATSUBARA K, HORITAZ, LANGDON T G. Exceptional superplasticity in an AZ61 magnesium alloy processed by extrusion and ECAP [J]. Mater Sci Eng A, 2006, 420(1–2): 240–244.
- [2] BARNETT M R, KESHAVARZ Z, BRRR A G, ATWEL D. Influence of grain size on the compressive deformation of wrought Mg-3Al-1Zn [J]. Acta Mater, 2004, 52(17): 5093–5103.
- [3] CHEN B, LIN D L, LI J, ZENG X Q, LU C. Equal-channel angular pressing of magnesium alloy AZ91 and its effects on microstructure and mechanical properties [J]. Mater Sci Eng A, 2008, 483–484:

- 113–116.
- [4] ZHENG M Y, XU S W, QIAO X G, WU K, KAMADO S, KOJIMA Y. Compressive deformation of Mg-Zn-Y-Zr alloy processed by equal channel angular pressing [J]. *Mater Sci Eng A*, 2008, 483–484: 564–567.
- [5] XIA K, WANG J T, WU X, CHEN G, GURVAN M. Equal channel angular pressing of magnesium alloy AZ31 [J]. *Mater Sci Eng A*, 2005, 410–411: 324–327.
- [6] VALIEV R Z, ISLAMGALIEV R K, ALEXANDROV I V. Bulk nanostructured materials from severe plastic deformation [J]. *Prog Mater Sci*, 2000, 45(2): 103–189.
- [7] MATSUBARA K, MIYAHARA Y, HORITA Z, LANGDON T G. Developing superplasticity in a magnesium alloy through a combination of extrusion and ECAP [J]. *Acta Mater*, 2003, 51(11): 3073–3084.
- [8] MUKAI T, YAMANOI M, WATANABE H W, HIGASHI K. Low temperature superplasticity of a fine-grained ZK60 magnesium alloy processed by equal-channel-angular extrusion [J]. *Scripta Mater*, 2001, 46(12): 851–856.
- [9] KIM W J, AN C W, KIM Y S, HONG S I. Mechanical properties and microstructures of an AZ61 Mg Alloy produced by equal channel angular pressing [J]. *Scripta Mater*, 2002, 47(1): 39–44.
- [10] KIM W J, HONG S L, KIM Y S, MIN S H, JEONG H T, LEE J D. Texture development and its effect on mechanical properties of an AZ61 Mg alloy fabricated by equal channel angular pressing [J]. *Acta Mater*, 2003, 51(11): 3293–3307.
- [11] EDDAHBI M, PEREZ P, MONGE M A, GARCES G, PAREJA R, ADEVA P. Microstructural characterization of an extruded Mg-Ni-Y-RE alloy processed by equal channel angular extrusion [J]. *J Alloys Compd*, 2009, 473(1–2): 79–86.
- [12] SHA G, LI J H, XU W, XIA K, JIE W Q, RINGER S P. Hardening and microstructural reactions in high-temperature equal-channel angular pressed Mg-Nd-Gd-Zn-Zr alloy [J]. *Mater Sci Eng A*, 2010, 527(20): 5092–5099.
- [13] HE S M, ZENG X Q, PENG L M, GAO X, NIE J F, DING W J. Microstructure and strengthening mechanism of high strength Mg-10Gd-2Y-0.5Zr alloy [J]. *J Alloys Compd*, 2007, 427: 316–323.
- [14] HUMPHREY F J, HATHERLY M. Recrystallization and related annealing phenomena [M]. Oxford: Elsevier Ltd, 2004: 285–319.
- [15] HUMPHREYS F J. Local lattice rotations at second phase particles in deformed metals [J]. *Acta Metall*, 1979, 27(12): 1801–1814.
- [16] HUMPHREYS F J, MILLER W S, DJAZEB M R. Microstructural development during thermomechanical processing of particulate metal-matrix composites [J]. *Mats Sci Technol*, 1990, 6(11): 1157–1166.
- [17] HUMPHREYS F J. The nucleation of recrystallization at second phase particles in deformed aluminium [J]. *Acta Metall*, 1977, 25(11): 1323–1344.
- [18] BALL E A, PRANGNELL P B. Tensile-compressive yield asymmetries in high strength wrought magnesium alloys [J]. *Scripta Metall Mater*, 1994, 31(2): 111–116.
- [19] MACKENZIE L W F, DAVIS B, HUMPHREYS F J, LORIMER G W. The deformation, recrystallization and texture of three magnesium alloy extrusions [J]. *Mat Sci Technol*, 2007, 23(10): 1173–1180.

等径角挤压处理后的 Mg-Gd-Y-Zr 合金的 微观组织和力学性能

张帆¹, 张可翔¹, 谭成文^{1,2}, 于晓东¹, 马红磊², 王富耻¹, 才鸿年¹

1. 北京理工大学 材料科学与工程学院, 北京 100081;

2. 中国航天员科研训练中心 先进材料行为特性实验室, 北京 100081

摘要: 研究等径角挤压过程中材料的微观组织和织构演变以及对其力学性能的影响。结果表明: 挤压 4 道次后的微观组织是不均匀的, 即在此过程中形成了粗晶区和细晶区 2 个区域。颗粒诱发的再结晶机制导致晶粒细化, 在 4 道次后形成了更加随机的织构。与挤压前的原始材料相比较, 经等径角挤压处理的材料虽然强度没有增加, 但是塑性有了显著的提高。用织构改变和第二相颗粒解释了合金塑性的变化。

关键词: Mg-Gd-Y-Zr 镁合金; 等径角挤压; 晶粒尺寸; 织构; 第二相颗粒; 力学性能

(Edited by YANG Hua)